Landslides (2018) 15:2267–2278
DOI 10.1007/s10346-018-1038-5
Received: 11 March 2018
Accepted: 3 July 2018
Published online: 16 July 2018

Karlis Kukemilks · Jean-Frank Wagner · Tomas Saks · Philip Brunner

Physically based hydrogeological and slope stability modeling of the Turaida castle mound

Abstract This study explores the potential of integrating state-of-the-art physically based hydrogeological modeling into slope stability simulations to identify the hydrogeological triggers of landslides. Hydrogeological models considering detailed morphological, lithological, and climatic factors were elaborated. Groundwater modeling reveals locations with elevated pore water pressures in the subsurface and allows the quantification of temporal dynamics of the pore water pressures. Results of the hydrogeological modeling were subsequently applied as boundary conditions for the slope stability simulations. The numerical models illustrate that the hydrogeological impacts affecting hillslope stability are strongly controlled by local groundwater flow conditions and their conceptualization approach in the hydrogeological model. Groundwater flow itself is heavily influenced by the inherent geological conditions and the dynamics of climatic forcing. Therefore, both detailed investigation of the landslide's hydrogeology and appropriate conceptualization and scaling of hydrogeological settings in a numerical model are essential to avoid an underestimation of the landslide risk. The study demonstrates the large potential in combining state-of-the-art computational hydrology with slope stability modeling in real-world cases.

Keywords Landslides · Numerical modeling · Hillslope hydrogeology · Preferential flow

Introduction

Elevated precipitation rates are typically associated with high pore water pressure and an increased risk of landslides (Knighton 1998; Uchida et al. 2001; Fox and Wilson 2010). Therefore, empirical relations between precipitation rates and landsliding or between the dynamics of the pore water pressure in landslide-affected slopes and slope ruptures have been established (Harp et al. 1990; McDonnell 1990; Knighton 1998). However, to consider the influence of groundwater on hillslope stability, a detailed understanding of the physical mechanisms on how groundwater affects the hillslope stability is required. Lourenço et al. (2006) conducted tests with artificial slopes in the laboratory which showed that increased pore water pressures are the main cause of slope ruptures, rather than internal erosion caused by the drag of slope particles (Lourenço et al. 2006).

Increase of the pore water pressures in hillslopes can be related to diverse hydrogeological mechanisms such as preferential flow, seasonally dependent perched water tables, and groundwater table fluctuations caused by rainfallor snowmelt. These effects are crucial for predicting the exact time and location of a landslide event. Several recent studies have focused on preferential flow, which can have a significant impact on hillslope stability by increasing the velocity and rate of groundwater flow by several orders of magnitude (Uchida et al. 2001; Anderson et al. 2009). No straightforward relation between preferential flow and slope stability has been established (Pierson 1983; Uchida et al. 2001). Local morphological, lithological, and climatic factors determine how hillslope stability is affected by preferential flow. Preferential flow can improve slope stability by draining groundwater and consequently reducing pore water pressures, but if due to rapid infiltration the transmissive capacity of a preferential flow path is exceeded or the groundwater conduit is blocked, preferential flow can also cause a rapid increase in the pore water pressures in the adjacent soil or rock matrix (Pierson 1983). When linking preferential flow with landslide activity, many studies focus on shallow landslides in the regolith cover of slopes (Sorbino and Nicotera 2013; Formetta et al. 2014; Kim et al. 2014). However, it has been shown that bedrock fractures can reduce hillslope stability as well (Padilla et al. 2014; Furuya et al. 2006; Gerscovich et al. 2006; Kukemilks et al. 2018).

Summarizing the main hydrogeological mechanisms affecting hillslope stability, Fox and Wilson (2010) propose the influence of pore water pressure on soil shear resistance, hydraulic gradient forces developing in steep slopes, and slope internal erosion caused by seepage flow. Additional effects of groundwater on hillslope stability are the surcharge of soil weight due to water infiltration and the increase of cohesion due to a negative pore water pressure (Lu and Godt 2013).

Slope stability models can in principle consider the aforementioned physical processes. Two inherently different approaches are available for the slope stability analysis. Firstly, the finite element method allows the determination of the distribution of the local safety factor in the hillslope (Griffiths and Lane 1999; Lu and Godt 2013). The alternative second approach, the limit equilibrium method, is a method that has been developed over the span of decades (Lu et al. 2012). Limit equilibrium approaches assume a rigid mass that is subject to implicit normal and shear stress distributions dictated by geometry. The use of finite elements provides an insight into the internal stresses between slices, which may or may not have a significant influence on stability.

Both 2D and 3D slope stability models have been elaborated for slope stability analysis (Baligh and Azzouz 1975; Kalatehjari and Ali 2013). In a 2D simulation, a three-dimensional landslide's geometry is reduced to a 2D slope section. The 2D analysis frequently results in an increased value of the safety factor (Gens et al. 1988), because the additional shear resistance of the sliding body, resulting from the end effects of the rupture surface, is neglected (Baligh and Azzouz 1975). 3D slope stability models are extended from 2D stability analysis by converting slices to columns (Kalatehjari and Ali 2013) or by applying 3D finite element simulators (Chen and Chameau 1983). For instance, a 3D analysis based on Fellenius' (Hovland 1977), Bishop's (Hungr 1987), or Morgenstern-Price's methods (Sun et al. 2012) is available. Typically, 3D slope stability methods assume a symmetrical failure surface with a predetermined shape (Kalatehjari and Ali 2013) such as a cylinder with conical or ellipsoidal ends (Baligh and Azzouz 1975), or a conical, wedge-shaped (Hovland 1977), or spherical (Cheng and Yip 2007) rupture surface. Moreover, the majority of

the 3D slope stability analysis methods are limited to symmetrical slopes where the landslide body is expected to move along the plane of symmetry (Kalatehjari and Ali 2013).

Despite a rapid increase of the accuracy of slope stability simulators, the impact of the preferential flow is neglected by most of the slope stability estimates (Shao et al. 2016). Slope stability models are able to consider various physical effects of groundwater affecting slope stability; however, the main problem remains in a correct identification of groundwater bodies in hillslopes. Observations of the groundwater table in borehole or simplified 2D groundwater simulators are not sufficient to analyze the effect of preferential flow or climatic impacts on the hillslope hydrogeology. Fully coupled, physically based hydrogeological models are tools which can provide insight into the dynamics of preferential flow processes. Shao et al. (2015, 2016) used a coupled hydrogeological-slope stability model to estimate the effect of preferential flow on hillslope stability. Preferential flow was conceptualized through a dual-permeability approach (Shao et al. 2015). The modeling showed no pronounced overall effect of groundwater on hillslope stability; however, preferential flow increased pore water pressures in the foot of slope, an effect which can contribute to landslides (Shao et al. 2015). Kukemilks et al. (2018) compared the effect of two preferential flow conceptualization approaches on hillslope stability. Dual-permeability and discrete fracture conceptualization approaches were used in a coupled hydrogeological and slope stability modeling (Kukemilks et al. 2018). When applying the dual-permeability conceptualization approach, no significant effect on the hillslope stability was determined (Kukemilks et al. 2018). However, when the groundwater flow in the discrete fracture was considered, groundwater discharging from the fracture caused elevated pore water pressures and a significant decrease of slope stability was observed (Kukemilks et al. 2018).

The literature above highlights the importance of preferential flow as well as flow conceptualization. While physically based models provide the quantitative framework to simulate such flow processes, they rarely have been applied to real-world studies. This study uses the latest advances in hydrogeological modeling to investigate the hydrogeological triggers of landslides and applies them to a slope stability simulation. Fully integrated, hydrogeological-slope stability modeling was conducted in a real-world study site of the Turaida castle mound (see Fig. 1). The 3D geological model was elaborated using the GeoModeller software and integrated into the hydrogeological simulations, where a large- and a small-scale hydrogeological model were compiled. The purposes of the large-scale model were to attain a general understanding of the groundwater distribution in the castle mound and to further apply in the slope stability estimate, model calibration, and delivering boundary conditions for a small-scale model. The small-scale model was applied for modeling of groundwater spring discharge on the hillslope which results from a discrete preferential flow path. Furthermore, the effects of a preferential flow path on hillslope stability were modeled. The hydrogeological simulations allowed the determination of the exact location and timing of critical groundwater heads causing the highest pore water pressures. The pressure heads from 3D hydrogeological modeling were imported in the slope stability model and the slope stability was estimated.

The study is structured in six sections. The "Introduction" section is followed by a study site description where the main geological settings and occurrence of previous landslides in the study area are described. The "Methodology" section explains parameter estimation procedure and subsequent model building and groundwater modeling. In the "Results" section, the hydrogeological responses are related to their climatic forcing functions. The triggers of landslides are identified. In the "Discussion" and "Conclusions" sections, in applying the results of numerical modeling, a detailed understanding of the hillslope hydrogeology and stability of the study site is attained.

Study area

The study site is located in the ancient Gauja River valley in central Latvia, on the western side of the Vidzeme Upland. During the last glacial age, the territory was covered by Scandinavian glaciers (Zelčs et al. 2011). Pleistocene glaciations, particularly the last Weichselian event, have formed the present-day relief (Zelčs and Markots 2004). As ice sheets retreated northwards during the end phase of the glacial age, glacier meltwaters were trapped between the retreating glacier margin and the Vidzeme Upland forming ice-dammed lakes. The drawdown of the ice-dammed lakes caused catastrophic flooding events (Zelčs and Markots 2004). Meltwater streams incised deep proglacial spillways forming the basis of the Gauja River valley and several of its tributary valleys (Zelčs et al. 2011). In the vicinity of the study area, the river valley reaches its maximal depth of up to 70 m (Zelčs and Markots 2004).

The climate in the study area is temperate, humid, and semi-continental, with an average annual temperature of − 5.5 °C in January and + 17 °C in July and an average annual precipitation of 700–800 mm (Kalniņa 1995). In the cold season, snowfall is frequent and can reach over 50 cm (Latvian Environment, Geology and Meteorology Centre 2013). Precipitation amounts can vary significantly in the study area. A recent extreme precipitation event occurred on 29 July 2014, when 122.8 mm of precipitation fell within 6 h (Latvian Environment, Geology and Meteorology Centre 2014).

In the Gauja River valley, an extensive gully erosion network, suffosion caves, and landslides are present (Āboltiņš 1995; Āboltiņš et al. 2011; Kukemilks and Saks 2013). In Latvia, landslides have mainly occurred on the slopes of river valleys (Veinbergs 1975; Mūrnieks 2002; Soms 2006; Āboltiņš et al. 2011; Kukemilks and Saks 2013). The Turaida castle mound is located in a landslide-susceptible area (Āboltiņš et al. 2011; Kukemilks and Saks 2013) on the bank of the Gauja River valley, separated by two gullies.

The Turaida medieval castle (see Fig. 1) in the Turaida Museum Reserve is an archeological and architectural monument and a popular tourist destination in the Baltic region (Turaida Museum Reserve 2012).

In February 2002, two dangerous landslides occurred in quick succession on the slopes of the Turaida castle mound. Landslides buried the local motor road and threatened the historic building. No people were injured or killed.

The first landslide (see Fig. 2) stretched about 90–95 m in length and was 35–38 m wide (Mūrnieks et al. 2002). This landslide constituted a severe threat to the historic building because its rupture surface was located only a few meters from the foundation. The second landslide followed the first approximately after 1 day and blocked the motor road at the foot of the castle mound. This landslide was only 25–27 m wide, but it extended 110 m downslope. The depth of the landslide reached 2–4 m. A third

Fig. 1 Overview of the Turaida medieval castle from north (The Turaida Museum Reserve 2012)

and much smaller landslide started forming at approximately the same time as the aforementioned two and continued for several weeks. Morphologically, it was similar to an earthflow (Mūrnieks et al. 2002).

In all three landslide cases, sliding occurred mostly in the uppermost soil layers and anthropogenic deposits. Pre-Quaternary deposits were only slightly affected (Mūrnieks et al. 2002). These landslide events were attributed to hydrogeological triggers, confirmed by several indications: landslides occurred after a long winter and intense snow melting leading to a high saturation of the sediments. Moreover, the landslides occurred at short intervals in different locations of the castle mound without any elevated seismic activity (Āboltiņš et al. 2011).

A section of the 3D geological model (see Fig. 3) illustrates the sediment sequences applied in the modeling. A detailed explanation of the 3D geological model building is described in the methodology section.

Under Quaternary deposits consisting mainly of glacial till and anthropogenic deposits, Middle and Upper Devonian sandstone, siltstone, and clay bedrock deposits form the geological basis of the castle mound (Āboltiņš et al. 2011). Quaternary series are located in the uppermost part of the mound reaching a maximum depth of 5 m. The upper layer in the Quaternary series consists of highly heterogeneous anthropogenic deposits. This sandy layer with an admixture of clay, organic compound, and construction materials was formed during different stages of the castle's construction and was relocated later during archeological excavations. Anthropogenic deposits can also be found on the slopes of the castle mound. The second Quaternary series in the stratigraphy of the castle mound is glaciogenic sandy loam with gravel and pebble admixture. The layer's thickness varies, reaching maximally 3 m, but in some locations it is not present (Mūrnieks et al. 2002).

The Devonian series mainly consists of alternating clay, silt, and poorly cemented sandstone layers. Thin clayey interlayers often dissect the sediment sequence (Mūrnieks et al. 2002).

Methodology

This study uses integrated hydrogeological and slope stability modeling to evaluate the landslide risk in a real-world study site. Initially, a 3D geological model using the GeoModeller software was compiled. A 3D geological model is necessary as a geological basis for the hydrogeological and slope stability simulations. The geological model was elaborated using boreholes, soundings, and results of geoelectrical and ground-penetrating radar investigation from the previous studies (Mūrnieks et al. 2002). LiDAR data compiled by Metrum (2013) were used to define the model's topography.

The layer surfaces from the 3D geological model were subsequently imported into the hydrogeological model. Groundwater modeling was conducted in two different spatial scales. A large-scale (surface area, 0.1 km^2) model was employed for calibration and investigating general hydrogeological settings of the whole castle mound, and a small-scale model (surface area: 0.04 km^2) was elaborated to simulate the local effects of preferential flow on a separated hillslope section. For groundwater modeling, the HydroGeoSphere (HGS) code was used (Aquanty Inc. 2013). HGS is a 3D fully coupled hydrological and hydrogeological simulator which allows to model surface, subsurface (for both saturated and unsaturated conditions), and fracture flow. This model has been used for solving complex problems concerning groundwater flow in the vadose zone (Banks et al. 2011; Schilling et al. 2014; Xie et al. 2014). Climatic forcing functions such as changing precipitation amounts, snowmelt, freezing, and thawing of soil are available in the model (Aquanty Inc. 2013; Brunner and Simmons 2012). A detailed description of the governing equations applied in the HGS code is discussed by Brunner and Simmons (2012) and is listed in the HGS user manual (Aquanty Inc. 2013).

In this study, integrated modeling of surface, subsurface, and fracture flow is conducted. Daily rainfall and snowmelt rates are implemented as boundary conditions.

The results of the hydrogeological simulation were used as boundary conditions for the limit equilibrium slope stability analysis. Critical pressure heads from hydrogeological simulation were imported in the slope stability model and safety factor of the selected hillslope sections determined.

Parameter estimation

The main hydrogeological modeling parameters in all domains are summarized in Table 1.

The hydraulic conductivities of the upper five layers were optimized using parameter estimation software (see detailed explanation in the "Hydrogeological Modeling" section). For the parameter estimation procedure, initial estimates of the hydraulic conductivities of the sediments were determined through pumping tests (Mūrnieks et al. 2002).

Additionally, for the hydrogeological simulation of the unsaturated zones α and β, the coefficients in the Van Genuchten saturation-pressure relation were estimated from the volumetric water content function applying the van Genuchten method (van Genuchten 1980). Rill storage height allows the consideration of the impact of ground surface microtopography in the surface/groundwater interaction. No surface flow can occur if the depth of surface water is smaller than the rill height. As the spring in the study site is covered by the regolith cover, no direct measurement of fracture aperture was available. Therefore, the characteristic groundwater bearing fracture aperture observed in the outcrops of sandstone deposits in the vicinity of the study area was applied in the model. It should be mentioned that the fracture apertures in

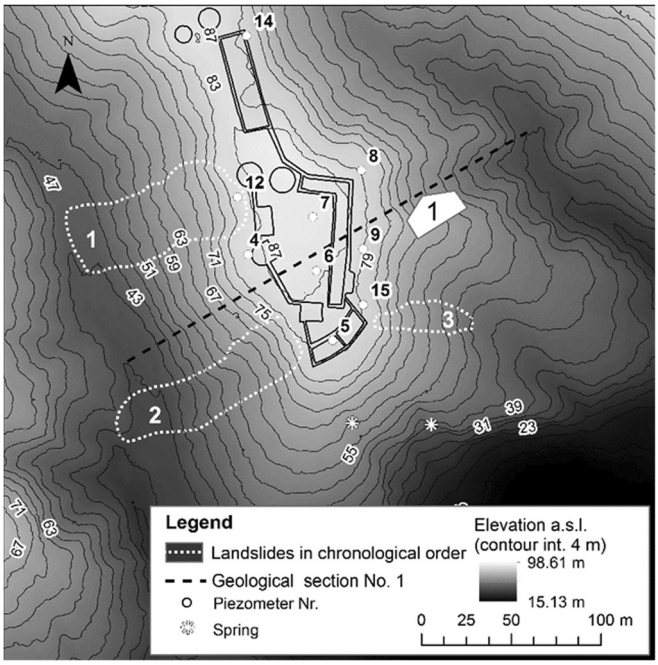

Fig. 2 Location of the landslides in the study site (compiled using (Mūrnieks et al. 2002; Metrum 2013))

the weak sandstone deposits in the outlet locations are enlarged by flowing water and can reach a width of several centimeters.

For the slope stability calculations, soil shear strength parameters determined through shear-box tests from the previous investigation (Mūrnieks et al. 2002) were applied. Additional tests were conducted in the soil mechanical laboratory of the University of Trier for determining previously unknown parameters of sandstone (see Table 2). Soil densities were determined applying the linear measurements method according to the ISO/TS 17892-2:2004 standard (Mūrnieks et al. 2002). The soil mechanical characteristics are summarized in Table 2.

Table 2 shows that the soil mechanical characteristics strongly depend on the place of sampling and the method of their estimation. Therefore, attempts were made to choose the most representative soil mechanical parameters (see Table 3). If several tests were conducted with the samples of a single layer, an average value was calculated from the available measurements. During the previous studies, the friction angle of sandstone was determined using the soil penetration test which provides only a correlated shear strength based on undrained measurements. To attain more reliable values, additional shear box tests were conducted with the sandstone samples to determine the drained friction angle. As the Devonian sandstone in the study site is very poorly cemented, it was not possible to obtain undisturbed samples, instead remolded samples were used. Applying a shear box test to such remolded samples results in a zero-cohesion value which is, however, very likely inaccurate. Consequently, the cohesion values from the in situ soil penetration test of the 3rd sandstone layer were preferred.

It should be added that the information concerning the soil mechanical parameters of the deepest layers was insufficient and consequently, identical values of friction angle and cohesion for the 4th, 6th, 8th and 10th clay layer and the 5th, 7th and 9th sandstone layer were applied.

According to the investigation results (Mūrnieks et al. 2002), the cohesion of the sediment layers is increasing in the core of the mound (Mūrnieks et al. 2002), probably due to lack of influences weakening cohesive bounds between soil particles, such as freezing and thawing or vegetation. However, no comparative measurements of the soil mechanical properties in the core and surface zone of the castle mound are available.

Hydrogeological modeling

Borders of the hydrogeological model domain were set along the talweg of two gullies on the eastern and western sides and the floodplain of the Gauja River in the southern part (see Fig. 1). Along the northwestern border, where a road is connecting the castle with the mainland, no significant groundwater exchange is to be expected (Mūrnieks et al. 2002).

Coupled modeling of groundwater flow in surface, subsurface, and fracture domains was conducted. Small- and large-scale hydrogeological models were elaborated to simulate hydrogeological conditions of the castle mound (see Fig. 4). The large-scale model was employed for the model's calibration and for investigating the general hydrogeological responses to climatic and geological factors. A small-scale model simulated the hillslope section where the discharge of a groundwater spring occurs.

Daily rainfall and snowfall amounts from the period between 1 January 2014 and 31 December 2015 were available from a meteorological observation station which is located approximately 2 km southwards from the study site in the town of Sigulda.

In the large-scale model, precipitation was conceptualized through first-type rainfall rate and snowmelt boundary condition. The depth of snow is controlled by the rates of snowfall, sublimation, and melting. Snowmelt rate is proportional to the snowmelt constant (η) and the difference between actual air temperature and threshold temperature equals 0 °C. If the actual air temperature $\leq$ 0°, $\eta = 0$ and no snow melting can occur (Aquanty Inc. 2013).

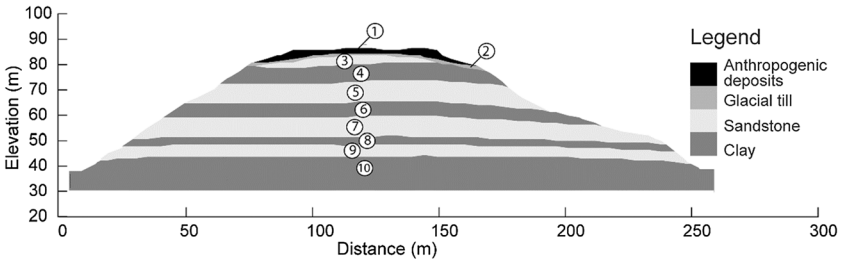

Fig. 3 Geological section no. 1 (see Fig. 1) illustrating the sediment layers (1–10) applied in the modeling

Table 1 Parameters of the hydrogeological modeling

Domain	Parameter	Anthropogenic deposits (1st layer)	Glacial till (2nd layer)	Sandstone (3rd/5th, 7th, 9th layer)	Clay (4th, 6th, 8th, 10th layer)
Subsurface	Hydraulic conductivity, K (m/s) (estimated, PEST)	2.34×10^{-6}	1.0×10^{-6}	$9.85 \times 10^{-6}/1.2 \times 10^{-5}$	1.50×10^{-10}
	Van Genuchten α, (m^{-1})	1	2	10	1
	Van Genuchten β	2	2	2.5	2
Surface	Manning's roughness coefficients, n_x and n_y ($m^{-1/3}s$)	0.6/0.6			
	Rill storage height, D_t (m)	0.005			
Fractures	Aperture (m)			0.005	

The rainfall rate and the snowmelt boundary allowed to sustain groundwater recharge in the model's domain. A critical depth boundary condition was set along the edge of the model's domain allowing water to leave the domain without changing the upstream groundwater heads or surface-water depths.

The small-scale model was elaborated to conduct detailed simulations for the hillslope section with the groundwater spring. A discrete fracture was introduced in the sandstone deposits to reproduce concentrated water discharge on the slope. The model was employed to attain a detailed insight into hillslope hydrogeology affected by preferential flow.

Without the rainfall rate and critical depth boundaries, the boundary condition of the prescribed groundwater head was set along the discrete fracture in the small-scale model. Elevation of the prescribed head was taken from the large-scale simulation when the maximum groundwater head in the location of the fracture was attained. This allows the consideration of the critical groundwater conditions in the hillslope stability modeling as it is expected that the maximal groundwater head will cause the highest saturation of hillslopes and maximum pore water pressures. A model containing discrete fractures allows the examination of the possible influence of groundwater discharging from groundwater conduits on the hillslope stability. Furthermore, both small- and large-scale models were applied to generate detailed hydrogeological boundary conditions for the subsequent slope stability modeling.

The hydraulic conductivities of the upper five layers were optimized using PEST (Doherty 2015). The PEST software uses Gauss Marquardt Levenberg parameter estimation with Broyden–Jacobian updating (Doherty 2015). The initial hydraulic properties were optimized in a steady-state simulation using average groundwater levels in the piezometers and the average precipitation rate. For a 2-year calibration period, piezometer observations in nine piezometer wells were provided by the Turaida Museum Reserve. Manual measurements with an average measurement frequency of 2 weeks were available. After the parameter optimization, a correlation coefficient of 0.82 between observed and modeled heads was attained.

The maximum and mean difference between observed and modeled groundwater heads is explicitly illustrated in Table 4. It should be considered that the homogeneous layer model for a hydrogeological simulation has limited applicability as the heterogeneity is emphasized in the castle mound. For instance, buried underground structures such as the foundations of former castle walls and another buildings are obviously affecting the groundwater flow conditions.

Table 2 Soil mechanical characteristics for slope stability modeling

Stratigraphy (m)	Depth of sampling (m)	Unit weight (kN/m^3) (Mūrnieks et al. 2002)	Cohesion (kPa) (shear box, Mūrnieks et al. 2002)	Cohesion (kPa) (soil penetration test, Mūrnieks et al. 2002)	Friction angle (°) (shear box, Mūrnieks et al. 2002)	Friction angle (°) (soil penetration test, Mūrnieks et al. 2002)
1. Anthropogenic deposits	0.6–0.85			26.72		23.17
2. Glacial till	0.85–1.00	21.65	18.30	44.80	28.80	21.00
	2.60–2.90		13.30		31.00	
3. Sandstone	3.00–4.40			4.89		32.44
4. Clay	5.00–5.30	20.77	146.70	64.10	11.30	24.90
	9.20–9.70		123.30		29.90	
5. Sandstone	13.30–17.20	20.70	0*		29.55*	
6. Clay	21.55–24.80	21.30				

*Determined in geotechnical laboratory of the University of Trier

Table 3 Soil mechanical properties applied in the simulation

Stratigraphy (m)	Unit weight (kN/m^3)	Cohesion (kPa)	Friction angle (°)
1. Anthropogenic deposits	21.65	26.72	23.17
2. Glacial till	21.65	15.80	29.90
3. Sandstone	20.70	4.89	29.55
4. Clay	20.77	135.00	20.60
5. Sandstone	20.70	4.89	29.55
6. Clay	21.30	135.00	20.60

Slope stability modeling

Several sections of the castle mound were selected for a slope stability analysis. A preliminary study with synthetic models was conducted to identify the most relevant factors affecting hillslope stability in the study site (Kukemilks et al. 2018). The synthetic hydrogeological model represents the typical lithological sequence with alternating conductive sandstone and less conductive clay layers at different slope angles. A discrete fracture network was applied in the sandstone layer to simulate the impact of water discharging from a fracture network on the hillslope stability (Kukemilks et al. 2018). The pore water pressures from the hydrogeological simulation were imported into the slope stability model. The modeling shows that slope angle is the factor affecting slope stability the most; however, pore water pressures, when discharging water from discrete fractures is considered, can reduce hillslope stability significantly as well (Kukemilks et al. 2018).

Consequently, sections of the Turaida castle mound with an elevated slope angle were selected for slope stability analysis. The small-scale model with groundwater discharging from the discrete fracture was elaborated. All the soil mechanical parameters in the small-scale analysis were kept identical as in the large-scale model. This allowed the isolation and measurement of the effect of discrete fracture discharge on hillslope stability. Pressure heads from the hydrogeological simulations were imported in the slope stability models. For each profile, two hydrogeological scenarios considering maximum and minimum groundwater heads of the whole simulation period were created. The minimum and maximum simulated groundwater heads were observed in June and August 2014 (see also Fig. 5).

The limit equilibrium analysis was applied to estimate the global safety factor of slopes. When using the limit equilibrium analysis, the landslide body is segmented in vertical slices and the force and moment equilibrium for each slice is determined. The failure plane with the minimum safety factor is determined through an iterative procedure (Lu and Godt 2013). In this study, the Morgenstern-Price method was applied, being one of the most complete limit equilibrium formulations (Lu et al. 2012; GEO-SLOPE International Ltd. 2015). Simplified methods such as Fellenius' or Bishop's formulations neglect some of the interslice forces that results in incomplete static equilibrium (Lu et al. 2012; GEO-SLOPE International Ltd. 2015). The Morgenstern-Price method satisfies both moment and force equilibrium principles and determines interslice normal and shear forces (Morgenstern and Price 1965). When Morgenstern-Price method is employed, a user-specified interslice shear to normal force function can be selected. In this study, half-sine function was applied which increases the interslice shear forces towards the middle of the landslide body (GEO-SLOPE International Ltd. 2015).

The entry range of the landslide in the slope stability model was specified over the plateau of the castle mound until the outcrop of first sandstone layer on the slope. The exit range extends starting from the first sandstone layer downslope until the foot of the slope. Because the entry range is significantly shorter as the exit range, 10 increments were selected over the entry range and 40 increments were specified over the exit range. The entry and exit ranges were selected to predict the formation of dangerous landslides which would reach the plateau of the castle mound and therefore could damage the structures of the Turaida castle. No formation of superficial landslides in the regolith cover of slopes or successive landslides starting at the foot of the slope and propagating upslope were considered in the modeling.

For section F, where the impact of groundwater discharging from the discrete fracture was considered (Fig. 9a), the entry range was set similarly as in the previous cases above the outcrop of the first sandstone layer, and the exit range below the sandstone. For the case when no preferential flow was considered (Fig. 9b), the entry and exit range of the landslide was constrained to one point to force the formation of slip surface in the same location as in Fig. 9a. This was necessary to compare the impact of preferential flow on hillslope stability when all other factors, such as slip surface entry and exit, and soil mechanical characteristics, were kept constant.

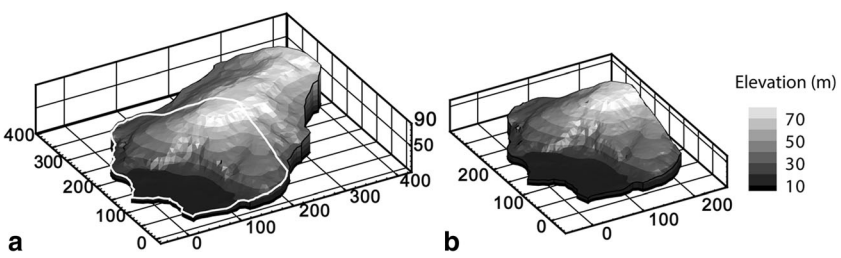

Fig. 4 Large (**4a**)- and small- (**4b**) scale hydrogeological models (white polyline indicates the boundary of the small-scale hydrogeological model)

Table 4 Maximum and mean difference between observed and modeled heads in nine observation wells

Piezometer No.	4	5	6	7	8	9	12	14	15
Depth (m)	3.43	2.78	3.90	5.40	2.15	3.85	5.65	2.50	2.82
Maximum difference (m)	1.06	0.53	0.84	0.85	1.65	1.53	1.23	1.99	1.48
Mean difference (m)	0.61	0.08	0.34	0.39	0.74	1.28	0.83	1.23	1.01

In the landslide simulation, initially a circular failure surface with 30 slices was applied and further optimized by incrementally altering separated segments of the slip surface (Greco 1996; GEO-SLOPE International Ltd. 2015). In the optimization process, the slip surface was divided into straight segments and the end points of each segment were moved randomly in an elliptical search area based on the Monte Carlo method. This procedure was applied for all points along the slip surface until the lowest safety factor was determined. Furthermore, the longest slip surface segment was divided into two parts and the optimization procedure was applied to the midpoint of the line segment (GEO-SLOPE International Ltd. 2015). This process was repeated until the factor of safety difference between two optimization iterations 1×10^{-7} was reached or 2000 optimization iterations were performed.

The SLOPE/W module allows the estimation of various effects of groundwater on hillslope stability such as buoyant and hydraulic gradient force, increased soil weight due to water infiltration, and the influence of negative pore water pressures (GEO-SLOPE International Ltd. 2015). The buoyant and hydraulic gradient forces are among the forces that decrease slope stability the most (Fox and Wilson 2010). The influence of increased soil weight due to infiltration varies depending on the location of the additional surcharge in the landslide profile. Negative pore water pressure or suction may improve slope stability by increasing the cohesion of soil; however, after heavy rainfall, the negative pore water pressure decreases rapidly (Lu and Godt 2013). Negative pore water pressure was not considered in the hillslope stability analysis because its effect strongly depends on changing climatic conditions. As its stabilizing effect decreases after precipitation events, stability increase due to negative pore water pressures was not applied for the estimation of slope safety.

Results

Hydrogeological modeling

To attain a general overview of the distribution of groundwater in the whole castle mound and model's calibration, the large-scale model was used. Further results from the large-scale modeling were applied as boundary conditions for a slope stability estimate of various hillslope sections in the castle mound. The small-scale model was employed to simulate preferential flow discharges on the hillslope. Furthermore, a separated slope stability model considering groundwater discharging from a preferential flow conduit was also used.

The climatic impact on the groundwater table changes generated in the large-scale simulation is explicitly illustrated in Fig. 5. The figure shows the daily simulated groundwater heads over a 2-year period from four observation points (corresponding with piezometer wells). The period of simulation from 1 January 2014 to 31 December 2015 was chosen due to the occurrence of severe precipitation events, these being namely: an extreme rain event on 29 July 2014, when the precipitation amount in 6 h attained 122.8 mm and in the beginning of 2015 when snow cover reacheded up to 32 cm on the study site (Latvian Environment, Geology and Meteorology Centre 2015).

A comparison of the dynamics of the modeled groundwater heads on the four observation points reveals that a rapid increase of the hydraulic heads follows the extreme precipitation of 29 July 2014. However, the highest groundwater heads are reached only approximately 1 month after the 29 July event.

The results of the small-scale hydrogeological modeling are illustrated in Fig. 6b. Water follows the fracture plane in sandstone deposits, because the less conductive clay layer prevents vertical infiltration and discharges from the groundwater conduit on the slope. After passing the thin clay interlayer, it infiltrates and rapidly saturates the lowermost sandstone and clay sediments.

Slope stability modeling

Six slope sections were chosen for the stability analysis (see Fig. 7). The sections A, B, C, D, and E were selected in locations with a relatively high slope angle as an indicator of potential landslide risk. Section F was set along the outlet of the spring to evaluate the possible slope instability caused by groundwater discharge on the slope of the castle mound.

Two large-scale hydrogeological scenarios were applied to the hillslope stability modeling in sections A, B, C, D, and F (see Fig. 7), comparing slope safety factor at the maximum and minimum groundwater heads during the modeling period (see Fig. 8). It should be added that, in the slope stability analysis, such impacts of groundwater on hillslope stability as increased weight due to soil saturation, buoyancy, and seepage forces were considered. The analysis did not consider an increase of cohesive strength due to negative pore water pressures.

Figure 8 illustrates the stability of four hillslope sections of the Turaida castle mound. In the figures, the rotation center of the most critical slip surface and its safety factor is shown. If the safety factor is less than or equal to one, slope rupture is to be expected.

Consequently, sections A and C are the most prone to landslides, as the modeling reveals a safety factor that indicates a high likelihood of slope rupture (see Fig. 7). An additional risk factor for section A is its proximity to the castle, exerting surcharge load in the top part of the hillslope section. The estimated weight of the castle's defense tower as equal to 1248 kN per meter was considered in the slope stability estimate. Section A in Fig. 7 shows the possible failure surface extending under the defense wall of the castle.

Figure 8 shows that, for scenarios A–D, very slight differences of slope stability calculated with the maximum and minimum groundwater heads can be observed.

The small-scale hydrogeological modeling was conducted to simulate the saturation of the hillslope by a discharging

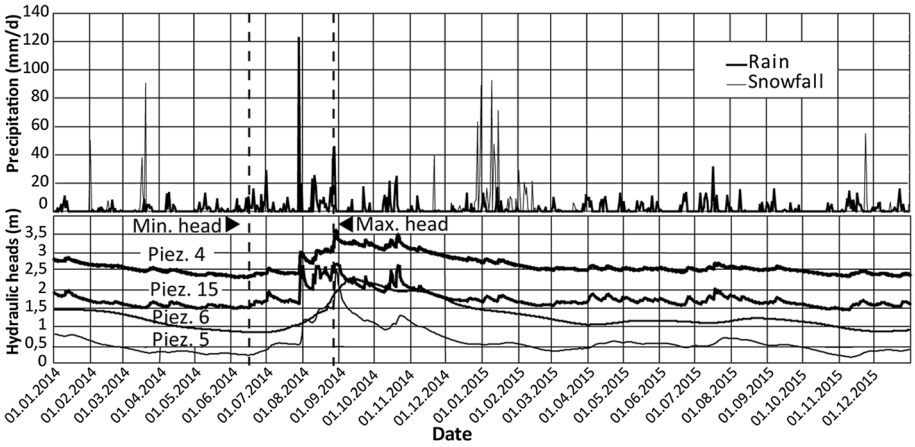

Fig. 5 Temporal changes of the rain, snowfall and groundwater heads in four selected piezometer wells from 1 January 2014 to 31 December 2015

groundwater spring. The reduction of the model's size has several advantages such as shorter simulation time, finer discretization of the model's geometry, and better convergence especially when simulating numerically challenging discrete fracture networks. In this scenario (Fig. 4b), a discrete fracture was introduced into the hydrogeological model, discharging in the outlet of the groundwater spring (see also Fig. 6).

Section F (see Fig. 7) was drawn through the outlet of the groundwater spring located on the southern side of the castle mound. In Fig. 9b, the entry and exit range of the landslide was set identical to that in Fig. 9a to determine the effect of preferential flow when all other factors were kept constant. In the scenario with preferential flow, a considerably lower slope stability (FS = 1.548) than without discrete fracture (FS = 2.162) can be observed.

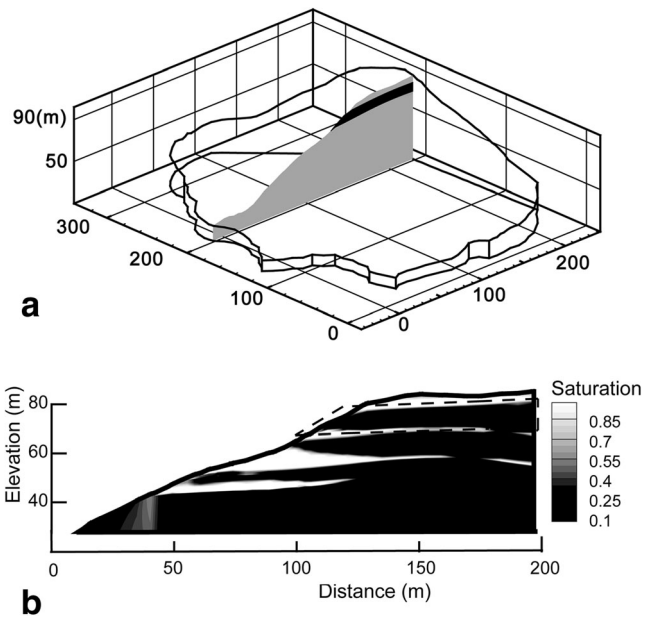

Fig. 6 Location of a discrete fracture in the small-scale model (the black plane in **a**) and an intense saturation of the hillslope caused by discrete fracture (marked by a dashed line in **b**)

Discussion

When analyzing the landslide-related factors, synthetic models have been employed to isolate separated related factors and evaluate their importance in hillslope stability. However, in a synthetic case, typically a limited number of factors are considered resulting in significant differences when compared to real-world conditions. This study attempted to integrate both hydrogeological and soil mechanical triggers contributing to landslide development in a real-world study site. The impact of climatic triggers such as rainfall and snowmelt was considered to simulate the effect of temporally variable climatic forcing functions on the landform development. Apart from a geomorphological viewpoint, the results of the modeling also illustrated the possible risks to the historical building after dangerous landslide events in the recent past.

The 3D geological and hydrogeological modeling allowed the identification of the most landslide-susceptible sections in the castle mound. Furthermore, the hillslope stability of the critical

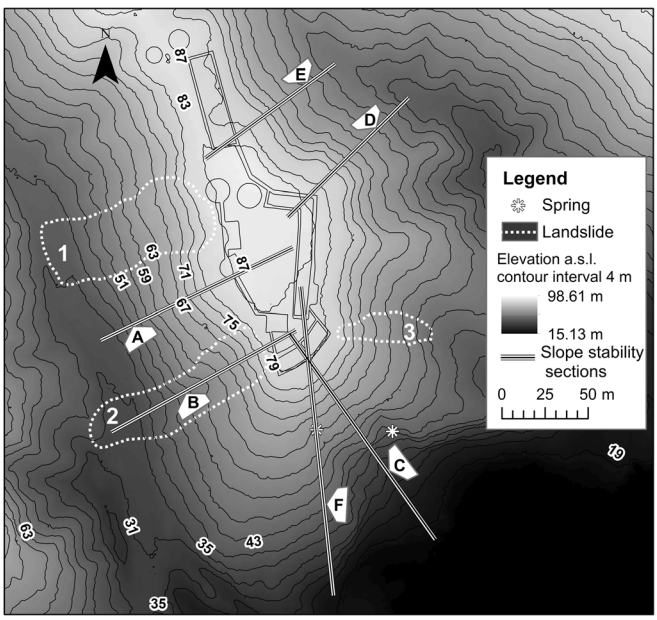

Fig. 7 Hillslope sections for the slope stability modeling

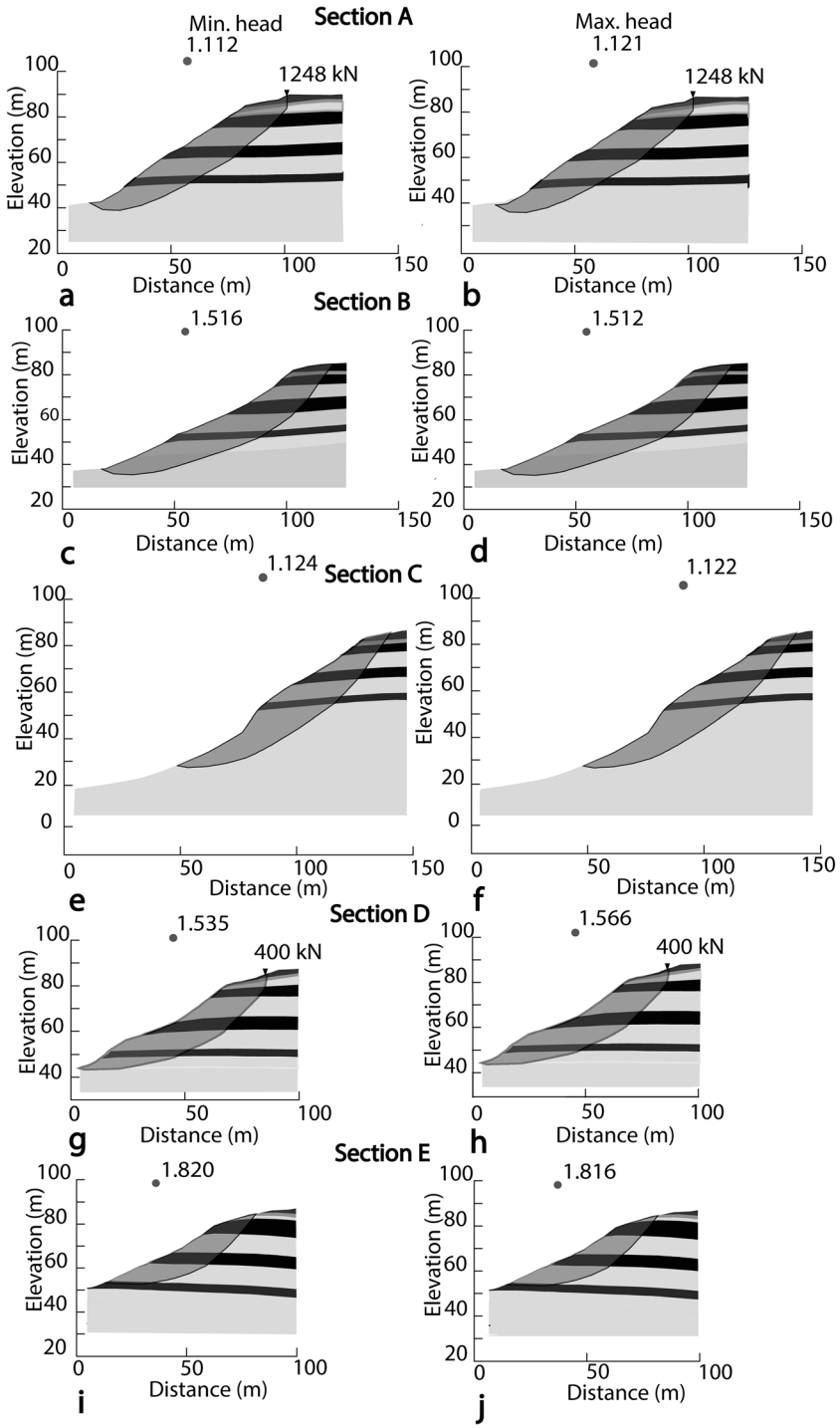

Fig. 8 The slope stability of four hillslope sections applying minimum and maximum groundwater heads from the large-scale simulation. **a**, **c**, **e**, **g**, **i** Slope safety factor calculated with the minimum groundwater heads. **b**, **d**, **f**, **h**, **j** Slope safety factor calculated by applying the maximum groundwater heads. The shaded segment indicates the landslide's slip surface with the lowest safety factor and (black circle) the rotation center of landslide

sections was estimated applying the 2D slope stability simulator. The 2D slope stability model was appropriate because a 3D slope stability simulation has limited applicability for the study site. The slopes of the castle mound have highly irregular morphology and therefore landslides are not expected to follow symmetrical shapes like cylindrical, ellipsoidal, or spherical failure surfaces as predicted by the 3D analysis. Moreover, for landslides with a low aspect ratio (depth to width), a flat 2D failure surface is more appropriate than a constrained 3D cylindrical or spherical shape.

For identifying the most critical sections for stability analysis, a preliminary study with synthetic models was conducted (Kukemilks et al. 2018). The synthetic models showed that slope angle and pore

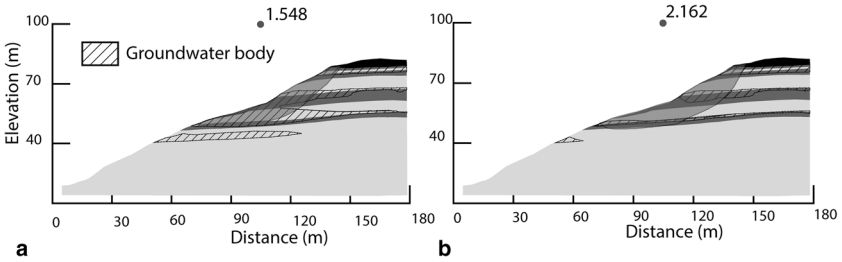

Fig. 9 The slope stability factor of section F, considering preferential flow from the small-scale hydrogeological simulation (**a**) and without preferential flow (**b**)

water pressures caused by groundwater discharging from discrete fractures are factors that decrease the hillslope stability most. To consider both aforementioned factors, 3D geological and hydrogeological modeling was conducted on two different scales. The large-scale model was employed for calibration and the simulation of the hydrogeological conditions of the whole castle mound. The small-scale model was employed for one single section of the castle mound to simulate discharging groundwater from a discrete fracture on the slope.

The steepest slope sections from the large-scale model were selected and their stability by the minimum and maximum groundwater heads was determined. In the small-scale model, one section through the outlet of the discrete fracture (spring) was selected and its stability calculated.

The integrated hydrogeological-slope stability modeling of selected sections shows that slope stability in different locations of the castle mound varies significantly. Section B on the SW slope (see Fig. 7) was selected in the location of a previous landslide to prove if a new landslide can occur in the location of a previous slide. Modeling shows that the stability in this section is sufficient and the formation of a new landslide in the previous location is not probable (see Fig. 8). Sections A and C have the lowest stability. One of the most slope stability decreasing factors in these sections is the steep slope angle. However, section C is narrow and located between two relatively flat hillslope precipices, exerting a stabilizing effect and preventing the formation of deep-seated landslides. Moreover, no significant structures are located directly on the upper part of this section, which could have exerted a surcharge load. However, the formation of shallow earthflow like slides and gully erosion is very likely. Contrariwise, a slope rupture in section A would have the most detrimental consequences because the structures of the Turaida castle are located very close to the slope edge. Moreover, this hillslope section is located between two previous landslides indicating possible landslide risk in the area. Therefore, additional investigations and possible slope stability improving measures are necessary. It should be added that the soil-mechanical parameters, especially of the lowermost layers, were not clear. Therefore, detailed parameter estimation in the study site would be useful for designing appropriate slope stabilization measures.

When analyzing the effect of groundwater on slope stability, geological and climatic forcings were playing an important role in the study site. An alternating sequence of conductive and less conductive layers leads to the formation of several perched water tables whose heads significantly depend on climatic conditions. Perching interlayers prohibit groundwater infiltration vertically, and instead groundwater follows above the less conductive layer and discharges on the hillslope. Concentrated groundwater discharge causes a local pore water pressure increase. Therefore the maximum groundwater heads were observed directly under the outlet of the upper less permeable layer which discharges into permeable sandstone resulting into a bulge of the groundwater table. Consequently, pore water pressure increases in the hillslope and slope stability is reduced. The perched water tables have high temporal variability, and moreover, the relation between groundwater heads and precipitation events is not straightforward. In the modeling period from 1 January 2014 to 31 December 2015, the highest modeled pore water pressures were attained approximately 1 month after the extreme precipitation event of 29 July. The most likely reason that the groundwater response lagged behind the precipitation event, is because the precipitation water was stored in the unsaturated zone. An additional factor leading to high modeled groundwater heads could have been the high overall precipitation amounts in the summer of 2014. As a result of several intense precipitation events, the groundwater heads were elevated over a long period of time resulting in water tables that were higher than from a single extreme precipitation event. No significant effect on the groundwater heads was observed after the intense snowfall and subsequent snowmelt at the beginning of 2015.

However, after comparing the slope safety factors of the five hillslope sections with the lowest and highest groundwater heads from the large-scale hydrogeological simulation, only a slight influence was observed. Contrariwise, when preferential flow paths were considered in the small-scale hydrogeological model, a significant effect of groundwater on hillslope stability was estimated. In the hydrogeological model, preferential flow was conceptualized as a discrete fracture discharging on the slope as a groundwater spring. Water discharging from the fracture saturated the lowermost sediments and reduced the hillslope stability. The aforementioned local scale effects affecting hillslope stability could not be considered if the generalized groundwater conditions, e.g., estimated groundwater table from piezometer wells, were applied. In geotechnical engineering, generalized groundwater conditions are frequently employed because small-scale analysis is very resource and time consuming. This can result in a slope stability overestimation. Therefore, in the study site, attention to local geological and hydrogeological settings should be paid to prevent unexpected slope failures.

An analysis of the small-scale hydrogeological factors is crucial from a geomorphological viewpoint as well. Thus, small-scale modeling considering climatic impacts and specific regional geological settings delivers an insight into the possible landform development of the region where the study site is located. Characteristic lithology consisting of weak sandstones dissected by less conductive clay and silt interlayers could have resulted in a common presence of erosional and mass wasting processes. Due to concentrated groundwater discharge above perching interlayers or from preferential flow paths, slope stability decreases in the affected zone resulting in landsliding and subsequent retrogressive gully

incision. In the longer term, this process could result in an abundant gully erosion network which is characteristic for the region of the study site (Āboltiņš 1995; Kukemilks and Saks 2013).

Conclusions

Recent advances in numerical groundwater simulators allow the development of detailed models of surface and subsurface flow in both porous and fractured media which allows the attainment of better understanding of the hydrogeological triggers of landslides. An integrated groundwater-slope stability modeling has a common application in several disciplines, such as geotechnical engineering and geomorphology, e.g., when designing earth buildings or investigating the climatic triggers of mass movements.

Most of the slope stability models have a focus on the soil mechanical part and the groundwater conditions are simplified which can result in a landslide risk underestimation. Moreover, depending on the modeling scale applied, hydrogeological effects on hillslope stability can vary significantly. This study is one of the first attempts to simulate the impact of small-scale hydrogeological factors such as fracture flow and extreme precipitation events on hillslope stability in a real-world study site. Additionally, in contrast to synthetic models, the real-world study site delivers a complete insight into landslide-related factors and their interactions. Results of large- and small-scale hydrogeological modeling show that the impact of the hydrogeological factors on hillslope stability can vary strongly depending on the local geological and climatic settings and their conceptualization approach in the numerical model. Choosing an appropriate modeling scale is crucial for considering local scale effects in the hydrogeological model.

When applying a discrete fracture preferential flow conceptualization approach in a small-scale model, hillslope stability is reduced significantly. Perching interlayers prohibit rapid hillslope drainage and thus the groundwater can accumulate in the hillslopes over longer time periods and result in elevated groundwater heads. Consequently, the whole lithological sequence of alternating conductive, fractured sandstones, and perching clay layers is susceptible to groundwater induced landsliding and gully erosion which could have contributed to the development of an abundant erosional network in the region.

Multiscale 3D hydrogeological modeling on the Turaida castle mound study site gives a reliable insight into the hydrogeological conditions of the site and their temporal variation. Moreover, by considering various scale groundwater conditions, the locations with the highest pore water pressures in the subsurface can be identified and applied as a hydrogeological boundary condition for a subsequent slope stability estimate. 3D hydrogeological models allow the observation of the reaction of a hydrogeological system to various climatic scenarios and prediction of possible landslide risks in the future under climate change.

Consequently, integrated hydrogeological and slope stability modeling is useful for the exact prediction of landslide events and understanding their triggers. This prevents an underestimation of landslide risk and allows the investigation of the impacts of climatic forcings on landform development.

Acknowledgements

We would like to thank Turaida Museum Reserve and personally Aivars Irbe for providing important modeling data, research assistant Fabien Cochand for the help with the modeling software, and Nelson Parker who provided linguistic corrections of the manuscript. We are grateful to our referees for the constructive reviews which helped to improve the article significantly.

Funding information

This work was supported by the Sciex NMS.CH program (grant number: 14.006); and German Academic Exchange Service (grant number: 57129429).

References

Āboltiņš O (1995) Gaujas Senleja. In: Kavacs G (ed) Latvijas Daba, 2nd Band. Latvijas Enciklopēdija, Rīga, p 101

Āboltiņš O, Mūrnieks A, Zelčs V (2011) Stop 2: the River Gauja valley and landslides at Sigulda. In: Stinkulis Ģ, Zelčs V (eds) Eighth Baltic stratigraphical conference. Post conference field excursion guidebook. University of Latvia, Rīga, pp 15–20

Anderson AE, Weiler M, Alila Y, Hudson RO (2009) Dye staining and excavation of a lateral preferential flow network. Hydrol Earth Syst Sci 13:935–944. https://doi.org/10.5194/hess-13-935-2009

Aquanty Inc. (2013) HydroGeoSphere: user manual, release 1.0. Waterloo, Ontario

Baligh M, Azzouz A (1975) End effects on stability of cohesive slopes. Journal of Geotechnical Engineering Division 101:1105–1117

Banks EW, Brunner P, Simmons CT (2011) Vegetation controls on variably saturated processes between surface water and groundwater and their impact on the state of connection. Water Resour Res 47(W11517). https://doi.org/10.1029/2011WR010544.

Brunner P, Simmons CT (2012) HydroGeoSphere: a fully integrated, physically based hydrological model. Ground Water 50:170–176. https://doi.org/10.1111/j.1745-6584.2011.00882.x

Chen RH, Chameau JL (1983) Three-dimensional limit equilibrium analysis of slopes. Géotechnique. 33:31–40. https://doi.org/10.1680/geot.1983.33.1.31

Cheng Y, Yip C (2007) Three-dimensional asymmetrical sloe stability analysis extension of Bishop's, Junbu's, and Morgenstern-Price's techniques. J Geotech Geoenviron 133(12):1544–1555. https://doi.org/10.1061/(ASCE)1090-0241(2007)133:12(1544)

Doherty J (2015) Calibration and uncertainty analysis for complex environmental models. Watermark Numerical Computing, Brisbane

Formetta G, Rago V, Capparelli G, Rigon R, Muto F, Versace P (2014) Integrated physically based system for modeling landslide susceptibility. Procedia Earth and Planetary Science 9:74–82. https://doi.org/10.1016/j.proeps.2014.06.006

Fox GA, Wilson GV (2010) The role of subsurface flow in hillslope and stream bank erosion: a review. Soil Sci Soc Am J 74:717–733. https://doi.org/10.2136/sssaj2009.0319

Furuya G, Suemine A, Sassa K, Komatsubara T, Watanabe N, Marui H (2006) Relationship between groundwater flow estimated by soil temperature and slope failures caused by heavy rainfall, Shikoku Island, southwestern Japan. Eng Geol 85:332–346. https://doi.org/10.1016/j.enggeo.2006.03.002

Gens A, Hutchinson J, Cavounidis S (1988) Three-dimensional analysis of slides in cohesive soils. Geotechnique 38:1–23. https://doi.org/10.1680/geot.1988.38.1.1

GEO-SLOPE International Ltd. (2015) Stability modeling with SLOPE/W: an engineering methodology, June 2015 Edition. Calgary, Alberta

Gerscovich DMS, Vargas EA Jr, de Campos TMP (2006) On the evaluation of unsaturated flow in a natural slope in Rio de Janeiro. Brazil Engineering Geology 88:23–40. https://doi.org/10.1016/j.enggeo.2006.07.008

Greco VR (1996) Efficient Monte Carlo technique for locating critical slip surface. J Geotech Eng 122:517–525. https://doi.org/10.1061/(ASCE)0733-9410(1996)122:7(517)

Griffiths DV, Lane PA (1999) Slope stability analysis by finite elements. Géotechnique 49:387–403. https://doi.org/10.1680/geot.1999.49.3.387

Harp EL, Wells WG, Sarmiento JG (1990) Pore pressure response during failure in soils. Geol Soc Am Bull 102:428–438. https://doi.org/10.1130/0016-7606(1990)102<0428:PPRDFI>2.3.CO;2

Hovland H (1977) Three-dimensional slope stability analysis method. Journal of Geotechal Engineering Division 103:971–986

Hungr O (1987) An extension of Bishop's simplified method of slope stability analysis to three dimensions. Geotechnique 37:113–117. https://doi.org/10.1680/geot.1987.37.1.113

Kalatehjari R, Ali N (2013) A review of three-dimensional slope stability analyses based on limit equilibrium method. Electron J Geotech Eng 18:119–134

Kalniņa A (1995) Klimats. In: Kavacs G (ed) Latvijas Daba, 2nd Band. Latvijas Enciklopēdija, Rīga, pp 247–251
Kim J, Lee K, Jeong S, Kim G (2014) GIS-based prediction method of landslide susceptibility using a rainfall infiltration-groundwater flow model. Eng Geol 182:63–78. https://doi.org/10.1016/j.enggeo.2014.09.001
Knighton D (1998) Fluvial forms and processes: a new perspective. Arnold, London
Kukemilks K, Saks T (2013) Landslides and gully slope erosion on the banks of the Gauja River between the towns of Sigulda and Ligatne. Estonian Journal of Earth Sciences 62:231–243. https://doi.org/10.3176/earth.2013.17
Kukemilks K, Wagner J-F, Saks T, Brunner P (2018) Conceptualization of preferential flow for hillslope stability assessment. Hydrogeol J 26:439–450. https://doi.org/10.1007/s10040-017-1667-0
Latvian Environment, Geology and Meteorology Centre (2013) Janvāris. Article, available online (accessed 02.01.2017): https://meteo.lv/lapas/laika-apstakli/klimatiska-informacija/latvijas-klimats/menesu-klimatiskaisraksturojums/janvaris/janvaris?id=1160&nid=541
Latvian Environment, Geology and Meteorology Centre (2014) Ekstremāli nokrišņi Siguldā 29. Jūlijā. Article, available online (accessed 05.01.2017): http://meteo.lv/jaunumi/laika-apstakli/ekstremali-nokrisni-sigulda-29-julija?id=768&cid=100
Latvian Environment, Geology and Meteorology Centre (2015) Observations. Data base, available online (accessed 25.01.2017): https://meteo.lv/en/meteorologija-datu-pieejamiba/?nid=697
Lourenço SDN, Sassa K, Fukuoka H (2006) Failure process and hydrologic response of a two layer physical model: implications for rainfall-induced landslides. Geomorphology 73:115–130. https://doi.org/10.1016/j.geomorph.2005.06.004
Lu N, Godt JW (2013) Hillslope hydrology and stability. Cambridge University Press, Cambridge
Lu N, Şener-Kaya B, Wayllace A, Godt JW (2012) Analysis of rainfall-induced slope instability using a field of local factor of safety. Water Resour Res. 48. https://doi.org/10.1029/2012WR011830
McDonnell JJ (1990) The influence of macropores on debris flow initiation. Q J Eng Geol Hydrogeol 23:325–331. https://doi.org/10.1144/GSL.QJEG.1990.023.04.06
Metrum SIA (2013) Lidar data, scanned in 2013
Morgenstern NR, Price VE (1965) The analysis of the stability of general slip surfaces. Géotechnique. 15:79–93. https://doi.org/10.1680/geot.1965.15.1.79
Mūrnieks A (2002) Turaidas pils stāv un stāvēs. Latvijas Ģeoloģijas Vēstis 10:2–6
Mūrnieks A, Meirons Z, Lācis A, Levins I (2002) Pārskats par Turaidas pilskalna, tā apkārtnes ģeoloģisko, hidroģeoloģisko un inženierģeoloģisko izpēti. Technical report. Latvian Environment, Geology and Meteorology Centre, Riga
Padilla C, Onda Y, Iida T, Takahashi S, Uchida T (2014) Characterization of the groundwater response to rainfall on a hillslope with fractured bedrock by creep deformation and its implication for the generation of deep-seated landslides on Mt. Wanitsuka, Kyushu Island. Geomorphology 204:444–458. https://doi.org/10.1016/j.geomorph.2013.08.024
Pierson TC (1983) Soil pipes and slope stability. Q J Eng Geol Hydrogeol 16:1–11. https://doi.org/10.1144/GSL.QJEG.1983.016.01.01.
Schilling OS, Doherty J, Kinzelbach W, Wang H, Yang PN, Brunner P (2014) Using tree ring data as a proxy for transpiration to reduce predictive uncertainty of a model simulating groundwater–surface water–vegetation interactions. J Hydrol 519:2258–2271. https://doi.org/10.1016/j.jhydrol.2014.08.063
Shao W, Bogaard TA, Bakker M, Greco R (2015) Quantification of the influence of preferential flow on slope stability using a numerical modelling approach. Hydrol Earth Syst Sci 19:2197–2212. https://doi.org/10.5194/hess-19-2197-2015
Shao W, Bogaard T, Bakker M (2016) The influence of preferential flow on pressure propagation and landslide triggering of the Rocca Pitigliana landslide. J Hydrol 543B:360–372. https://doi.org/10.1016/j.jhydrol.2016.10.015
Soms J (2006) Regularities of gully erosion network development and spatial distribution in south-eastern Latvia. Baltica 19:72–79
Sorbino G, Nicotera MV (2013) Unsaturated soil mechanics in rainfall-induced flow landslides. Eng Geol 165:105–132. https://doi.org/10.1016/j.enggeo.2012.10.008
Sun G, Zheng H, Jiang W (2012) A global procedure for evaluating stability of three-dimensional slopes. Nat Hazards 61:1083–1098. https://doi.org/10.1007/s11069-011-9963-9
The Turaida Museum Reserve (2012) The Historical Centre of Turaida, The Turaida Museum Reserve: a guide. Jurkāne A (ed). Mantojums Publishing House, Rīga, 2012, 160 pp
Uchida T, Kosugi K, Mizuyama T (2001) Effects of pipeflow on hydrological process and its relation to landslide: a review of pipeflow studies in forested headwater catchments. Hydrol Process 15:2151–2174. https://doi.org/10.1002/hyp.281
van Genuchten MT (1980) A closed-form equation for predicting the hydraulic conductivity of unsaturated soils. Soil Sci Soc Am J 44:892–898
Veinbergs I (1975) Formirovanie Abavsko-Slotsenskoj sistemy dolin stoka talykh lednikovykh vod. In: Danilāns I (ed) Voprosy chetvertichnoj geologii. Zinātne, Rīga, pp 82–102 (in Russian, with English Abstr.)
Xie Y, Cook PG, Brunner P, Irvine DJ, Simmons CT (2014) When can inverted water tables occur beneath streams? Groundwater 52:769–774. https://doi.org/10.1111/gwat.12109
Zelčs V, Markots A (2004) Deglaciation history of Latvija. In: Ehlers J, Gibbard PL (eds) Quaternary glaciations—extent and chronology, part I: Europe. Elsevier B.V, Amsterdam, pp 225–243
Zelčs V, Markots A, Nartišs M, Saks T (2011) Pleistocene glaciations in Latvia. In: Ehlers J et al (eds) Developments in quaternary science. Quaternary glaciations—extent and chronology. A closer look, vol 15. Elsevier B.V, Amsterdam, pp 221–229

K. Kukemilks (✉) · **J.-F. Wagner**
Lehrstuhl für Geologie,
Universität Trier,
Behringstraße 21, 54296, Trier, Germany
Email: kukemilks.karlis@inbox.lv

J.-F. Wagner
e-mail: wagnerf@uni-trier.de

T. Saks
Department of Geosciences,
University of Fribourg,
Chemin du Musée 4, CH-1700, Fribourg, Switzerland
e-mail: tomas.saks@unifr.ch

P. Brunner
Centre d'Hydrogéologie et de Géothermie (CHYN),
Université de Neuchâtel,
Rue Emile Argand 11, CH-2000, Neuchâtel, Switzerland
e-mail: philip.brunner@unine.ch